Measurements of the Critical Power for Self-Injection of Electrons in a Laser Wakefield Accelerator

D. H. Froula,[1,*] C. E. Clayton,[2] T. Döppner,[1] K. A. Marsh,[2] C. P. J. Barty,[1] L. Divol,[1] R. A. Fonseca,[4] S. H. Glenzer,[1] C. Joshi,[2] W. Lu,[2] S. F. Martins,[4] P. Michel,[1] W. B. Mori,[2] J. P. Palastro,[1] B. B. Pollock,[1,3] A. Pak,[2] J. E. Ralph,[1,2] J. S. Ross,[1,3] C. W. Siders,[1] L. O. Silva,[4] and T. Wang[2]

[1]*L-399, Lawrence Livermore National Laboratory, P.O. Box 808, Livermore, California 94551, USA*
[2]*Department of Electrical Engineering, University of California, Los Angeles, California 90095, USA*
[3]*Department of Mechanical and Aerospace Engineering, University of California, San Diego, 9500 Gilman Drive, La Jolla, California 92093, USA*
[4]*GoLP/Instituto de Plasmas e Fusão Nuclear, Instituto Superior Técnico, Lisbon, Portugal*

(Received 17 June 2009; published 19 November 2009)

A laser wakefield acceleration study has been performed in the matched, self-guided, blowout regime producing 720 ± 50 MeV quasimonoenergetic electrons with a divergence $\Delta\theta_{\mathrm{FWHM}}$ of 2.85 ± 0.15 mrad using a 10 J, 60 fs 0.8 μm laser. While maintaining a nearly constant plasma density (3×10^{18} cm^{-3}), the energy gain increased from 75 to 720 MeV when the plasma length was increased from 3 to 8 mm. Absolute charge measurements indicate that self-injection of electrons occurs when the laser power P exceeds 3 times the critical power P_{cr} for relativistic self-focusing and saturates around 100 pC for $P/P_{\mathrm{cr}} > 5$. The results are compared with both analytical scalings and full 3D particle-in-cell simulations.

DOI: 10.1103/PhysRevLett.103.215006 PACS numbers: 52.38.Kd, 41.75.Jv, 52.35.Mw

Thirty years ago, Tajima and Dawson predicted that an intense laser pulse can drive a plasma wake to produce 10–100 GeV/m electric fields which could accelerate electrons [1]. More than a decade later, laser-accelerator experiments used laser beat waves and the Raman forward instability to drive large amplitude plasma waves that generated electron beams with a continuous spectrum reaching high energies [2–6]. It was not until the laser technology advanced to having a sufficiently short pulse duration, at powers above 10 TW, that ~100 MeV quasimonoenergetic electron beams accelerated by laser-produced wakefields were realized [7–9].

The ponderomotive force of the rising edge of an ultrashort ($\tau \sim 2\pi/\omega_p$) relativistically intense laser pulse propagating through an underdense plasma can completely blow out the electrons forming a spherical ion bubble around the pulse of the laser [10,11]. Here, ω_p is the plasma frequency. Electrons along the sheath of this bubble are pulled towards the laser axis and cross at the rear. Electrons residing within the region of high-accelerating and focusing fields can be self-injected into the accelerating structure if they gain enough velocity to catch up with the phase velocity of the wake driven by the laser. These self-injected electrons are then accelerated until they either outrun the slower moving accelerating potential of the wake over a ''dephasing length'' L_{dp} or the laser intensity is reduced so that no significant wake is excited. In order to maintain the intensity of the laser pulse over many Rayleigh lengths Z_r (typically $Z_r \ll L_{\mathrm{dp}}$), the diffraction of the laser field must be compensated by the refraction within the self-generated electron density channel of the wake [12–16] or an external waveguide [7].

The dephasing length (and therefore the electron energy) of a laser wakefield accelerator (LWFA) can be increased by reducing the electron plasma density since $L_{\mathrm{dp}}[\mathrm{cm}] \simeq (\frac{P}{\mathrm{TW}})^{1/6}(\frac{10^{18}\ \mathrm{cm}^{-3}}{n_e})^{4/3}$ [13]. However, for effective self-guiding and self-injection, the laser power must be maintained well above the critical power P_{cr} for self-focusing given by $P_{\mathrm{cr}} = 17\omega_0^2/\omega_p^2\mathrm{GW}$, where ω_0 is the laser frequency [13]. Simulations have suggested a power threshold for self-injection at low electron densities ($n_e \sim 10^{18}$ cm^{-3}) to be around $P/P_{\mathrm{cr}} = 4$–8 [13,17], but this has not been experimentally demonstrated. Previous experiments in capillary discharge plasmas at low densities have shown thresholds for self-trapping [18] and ionization assisted self-trapping [19,20]. A study of the trapping threshold at high densities (low electron beam energies) was also performed in gas jets [5], but there have been no measurements of this threshold at $n_e < 5 \times 10^{18}$ cm^{-3} without an external guiding structure. At these low densities, laser pulses from high-power Ti:sapphire lasers with a typical pulse duration of about 50 fs are completely contained within the ion bubble and the electrons are accelerated to high energies.

In this Letter, we present the first GeV-class laser wakefield acceleration experiments where a self-injection threshold is demonstrated for densities below 5×10^{18} cm^{-3} in a gas jet without a guiding structure. For these densities, the laser power and spot size are such that a fully blown out self-guiding accelerating structure is excited over 8 mm of plasma and the laser pulse is contained within this bubble. The charge in the electron beams increases rapidly from 0.1 pC to a saturation level of ~100 pC when P/P_{cr} is increased from 3 to 5.

 © 2009 The American Physical Society

Furthermore, the energy of the electron beam is measured to increase from 75 to 720 MeV when the plasma length is increased from 3 to 8 mm. These results are supported by full 3D particle-in-cell (PIC) simulations and are also consistent with theoretical predictions [13].

The experiments reported here were performed at the Jupiter Laser Facility, Lawrence Livermore National Laboratory, using the 200 TW Ti:sapphire Callisto Laser System. To maintain the short laser pulses ($\tau_{\mathrm{FWHM}} = 60 \pm 5$ fs), the system employs an optical pulse shaper [21]. Figure 1 shows the experimental setup where the laser beam was focused by an $f/8$ off-axis parabola to the leading edge of a He gas jet. The vacuum spot size w_0 was measured at low powers to be 15 μm at the $1/e^2$ intensity point which corresponds to a $Z_r = \pi w_0^2/\lambda = 900$ μm. The total power contained within the central spot is measured to be 30%, and all powers quoted in the Letter take this into account. The fraction of energy outside of the central spot is not expected to contribute to the wakefield excitation—a highly nonlinear effect.

Three supersonic gas jets were designed to produce near-uniform density profiles over 3, 5, and 8 mm [22]. The density increased approximately linearly from vacuum to the plateau density over 500 μm. The density profiles were characterized using low laser powers to ionize the He gas and a Lloyd mirror interferometer that employed a 100 fs probe beam. The error in the absolute density of the plateau is estimated to be $\pm 1 \times 10^{18}$ cm^{-3} [14].

The electron beams produced by this laser wakefield accelerator were characterized using the two-screen spectrometer shown in Fig. 1 which provides an accurate measurement of the electron charge, divergence, energy, and deflection [23]. The electrons propagating out of the plasma pass through a 40 μm thick aluminum optical beam dump and a 62.5 μm thick Mylar vacuum window before being deflected by a 20-cm-long 0.46 Tesla magnetic field. Electrons with sufficient energies to propagate through the magnet are detected by two successive image plates providing a unique solution to their energy and exit deflection angle through the relativistic equations of motion [24]. Furthermore, the image plates have been calibrated to provide a direct measure of the electron charge [25]. For electron energies of interest in this study (above 25 MeV), the system can detect less than 1 fC of charge within a 35 mrad collection angle.

Figure 2 shows that charge is self-injected and accelerated to high energies when $P/P_{\mathrm{cr}} \gtrsim 3$. The data shown in this plot span a range of peak laser powers (5–100 TW) and two plasma densities. Below the critical power for self-injection, less than 1 fC of charge is detected at energies above 250 MeV while above this threshold, the charge increases rapidly and saturates at about 100 pC. The charge measured in these experiments can be characterized as having three spectral features which are evident in the spectra shown in Fig. 1: a low-energy <50 MeV continuous spectrum as seen on IP3, a low-energy 25–150 MeV peak as seen in Fig. 1(b), and a >250 MeV high-energy peak as seen in Fig. 1(c). The low-energy continuous spectrum has a large divergence and is therefore not cor-

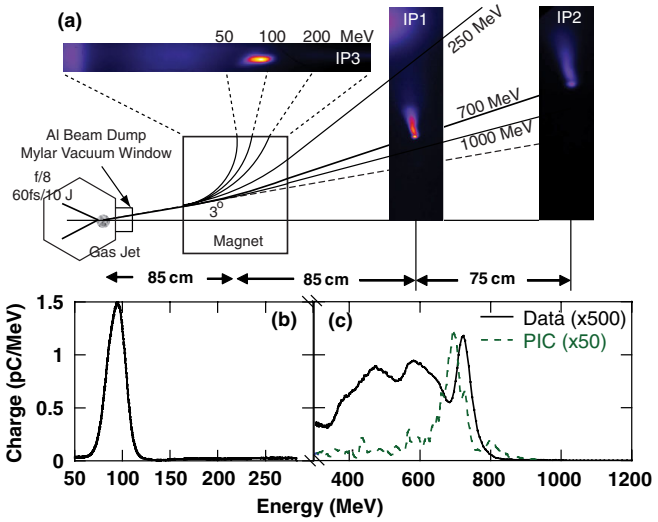

FIG. 1 (color online). (a) A schematic of the experiment. Two successive image plates (IP1, IP2) are used to measure both the energy of the electrons and their deflection from the laser axis. Low-energy electrons ($E \lesssim 150$ MeV) are deflected out of the top of the magnet and are detected by a third image plate (IP3). The spectra show results from an experiment where a peak power of 65 TW produced a 720 ± 50 MeV electron beam with a 3° deflection; a 90 ± 10 MeV feature is also measured on IP3. The electron spectra measured by IP3 and IP1 are shown in (b) and (c), respectively. The total charge in the 90 MeV feature was measured to be 34 and 6.7 pC for energies above 300 MeV. The high-energy spectra are compared with PIC simulations (dashed curve).

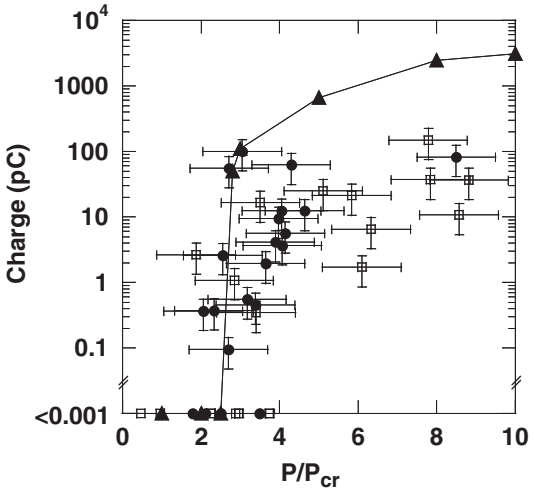

FIG. 2. The total charge accelerated above 250 MeV is shown as a function of P/P_{cr} at two densities: 3×10^{18} cm^{-3} (●) and 5×10^{18} cm^{-3} (□). Below $P/P_{\mathrm{cr}} < 3$, no charge is accelerated beyond 250 MeV. The PIC simulations (▲) agree well with the measured self-injection threshold. The open (closed) symbols represent results from the 5-mm (8-mm) -long gas jets.

rectly resolved by our spectrometer. This part of the spectrum has been subtracted from all charge measurements.

The open symbols in Fig. 3 show that, as the gas-jet length is increased from 3 to 8 mm, the electron beam energy is increased by nearly an order of magnitude. Here, the dephasing length is held constant at 4.5 mm by maintaining a constant laser power and plasma density. Furthermore, a second data set is shown (solid squares) where the electron energy was further increased by adjusting the density so that the dephasing length approximately equaled the acceleration length. Here, the acceleration length $L_{\rm acc}$ is the gas-jet length minus the length over which the laser spot evolves to its matched spot size as seen in the simulations ($L_{\rm evl} \simeq 2.5$ mm). The agreement between the dephasing-limited energy gain given by the expression $E[\mathrm{MeV}] \simeq 115 P[\mathrm{TW}]^{1/4} L_{\rm acc}[\mathrm{mm}]^{1/2}$ [13] and the experimentally observed energies is reasonable. The data point at 720 MeV, where $L_{\rm acc} = 5$ mm, indicates that the nearly self-matched laser spot is guided over 8 mm ($\sim 10 Z_r$). The divergence $\Delta\theta_{\rm FWHM}$ of the 720 MeV feature seen on IP1 is 2.85 ± 0.15 mrad and compares well with the 2 mrad results seen in the simulations. Monte Carlo simulations using the code ITS [26] indicate that the electron divergence resulting from the scattering through the aluminum optical beam dump, the Mylar vacuum window, and 120 cm of air is <0.25 mrad for an electron energy of 700 MeV. Using the source size measured from the simulations ($\sigma_r \simeq 1$ μm), the corresponding normalized emittance $\epsilon_N = \sigma_r \gamma \Delta\theta_{\rm FWHM}$ is estimated to be 5 mm-mrad.

Particle-in-cell simulations were performed in 3D using the code OSIRIS [27] and initialized with the experimental parameters. The initial He gas profile consistent with the measured 8 mm density plateau was used. The simulations used a 100 μm $\times$ 150 μm $\times$ 150 μm computational window corresponding to $4000 \times 256 \times 256$ grid points with a resolution along the laser propagation direction of 25.4 and 595 nm in the transverse plane and had four particles per cell.

Figure 4 shows PIC simulation results where the laser beam completely blows out the electrons producing a stable accelerating structure. In these simulations, it is evident that the laser pulse is nearly matched to the plasma conditions in that the laser pulse is completely contained within the ion bubble and continues to be guided over the entire length of the plasma. The laser beam is focused at the edge of the density plateau and initially self-focuses over the first 700 μm to a radius of 8 μm before expanding over a few vacuum Rayleigh lengths to the matched laser spot size $w_m[\mu\mathrm{m}] \cong 8.5 \times 10^6 (P[\mathrm{TW}])^{1/6} \times (n_e[\mathrm{cm}^{-3}])^{-1/3} \cong 13 \mu$m.

The injection of electrons occurs predominantly in two stages. The first group of electrons are injected when the laser initially overfocuses. However, this group contains a small fraction of the total charge. Once the laser pulse reaches its matched diameter, after about 2.5 mm of propagation, electrons begin to be continuously injected into the first bucket. These electrons constitute the majority of the charge accelerated to high energies. After an additional 4.5 mm of propagation, this second group of injected electrons begin to dephase with the wake (i.e., rotating in phase space) and exit the plasma with a quasimonoenergetic feature at about 700 MeV [Fig. 1(c)].

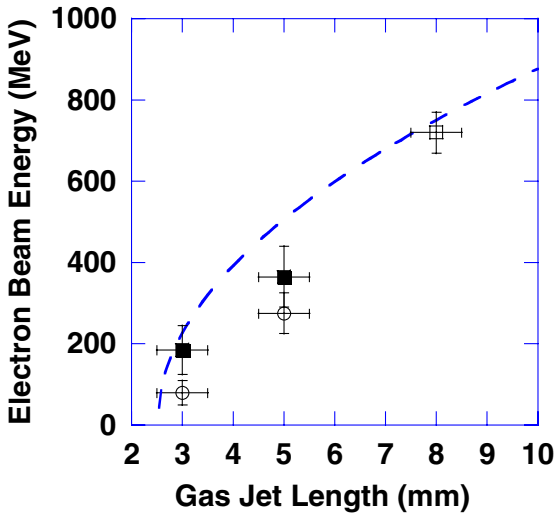

FIG. 3 (color online). The measured energy as a function of plasma length is plotted for a fixed plasma density of 3×10^{18} cm^{-3} and a peak laser power in the central spot of 65 ± 15 TW (○). The energy at each gas-jet length was optimized (■) by changing the plasma density (from 3×10^{18} cm^{-3} to 9×10^{18} cm^{-3} for the 3-mm gas-jet length and to 6×10^{18} cm^{-3} for the 6-mm gas-jet length) so that the dephasing length is nearly equal to the acceleration length (see text). This increased the measured energy from the open circles to the closed squares. Also shown is the maximum calculated energy (dashed line) for electrons injected after the pulse evolution distance of 2.5 mm.

In order to find the self-injection threshold, numerous PIC simulations were necessary. Therefore, a recently developed capability was used that allows for the computation to be performed in a boosted frame [28,29]. For our parameters, choosing a boosted-frame Lorentz factor of 5 provided a factor of 20 reduction in simulation time. This allowed us to perform many simulations, eight of which are shown in Fig. 2. The boosted frame simulations have been benchmarked in this parameter regime against simulations performed in the lab frame and agree to better than 10%. In particular, a simulation in the full laboratory frame was performed, using the exact conditions of the experiment, and reproduced both the charge and spectrum observed in the boosted frame simulations.

The electron charge accelerated above 250 MeV in the simulations and the experiments is compared in Fig. 2. Although the simulations reproduce the electron injection threshold, they quickly overestimate the charge accelerated to high energies as the laser power is increased. We speculate that this could be a result of the inevitable imperfections present in high-power laser spots or density variations in the gas-jet profiles.

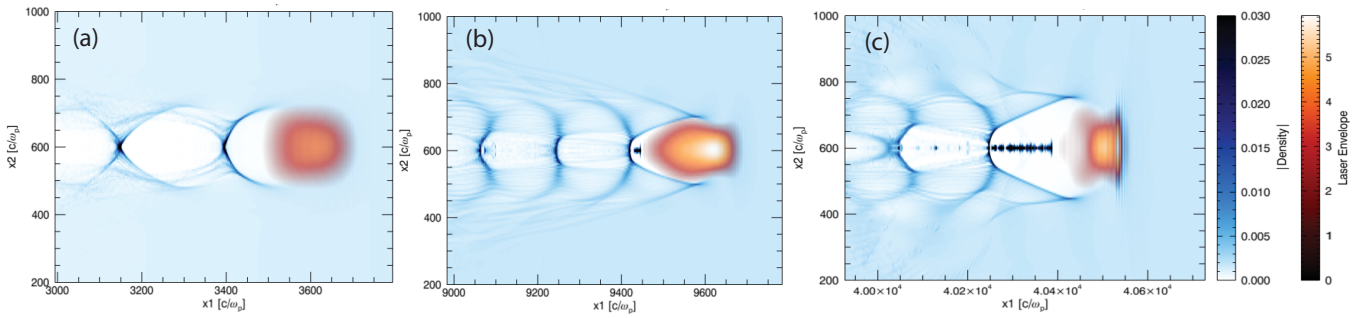

FIG. 4 (color online). (a) Snapshots of the density profiles (blue color table online) from the simulation are shown initially at $z = 0.5$ mm, where the laser pulse has completely blown out the electrons forming a nearly spherical wakefield. (b) As the laser pulse evolves, a stable accelerating structure is formed and self-injection occurs ($z \sim 3$ mm). (c) By the end of the plasma ($z = 8.5$ mm), the highest energy electrons have begun to dephase, producing a 700 MeV electron beam. The laser pulse is superimposed on the density map (red color table online).

A physical picture for how electrons are self-injected into a plasma wakefield in the blowout regime has been developed and verified in simulations [13]. Provided the blowout radius is large [$R_b \simeq 2k_p^{-1}\sqrt{a_0} \sim (3\text{–}4)k_p^{-1}$, where $\omega_p = ck_p$ and a_0 is the normalized vector potential], electrons are always injected for the range of plasma densities of interest to laser wakefield accelerators. In this regime, relativistically intense wakes are formed and the electrons crossing at the back of the bubble will have a forward velocity close to the speed of light and become injected. In the matched case, where $R_b \simeq w_m \sim 2\sqrt{2}k_p^{-1}(P/P_{\rm cr})^{1/6}$, the electron injection threshold is given by $P/P_{\rm cr}$ in the range of 1.4–8 (for k_pR_b of 3–4, respectively). The exact value of this threshold will depend on the actual laser profile, plasma density uniformity, etc. However, the observed self-injection threshold reported here is consistent with our current understanding of trapping in 3D nonlinear wakes.

In summary, we have used a 200 TW short-pulse laser to demonstrate a threshold for electron self-injection ($P/P_{\rm cr} \simeq 3$) at low densities (3×10^{18} cm^{-3}) in a self-guided laser wakefield accelerator experiment. The electron energy gain was measured to monotonically increase with plasma length, from 75 MeV at 3 mm to 720 MeV at 8 mm. The combination of the high-electron-beam energy with a low emittance ($\epsilon_N = 5$ mm-mrad) suggests that our experiments produced a stable guiding and accelerating structure which is also seen in full three-dimensional PIC simulations.

We would like to thank B. Stuart, D. Price, S. Maricle, and J. Bonlie for their contributions to upgrading the Callisto Laser System for this experiment. This work was performed under the auspices of the U.S. Department of Energy by Lawrence Livermore National Laboratory under Contract No. DE-AC52-07NA27344 and a Department of Energy Grant No. DEFG03-92ER40727 (UCLA) and was partially funded by the Laboratory Directed Research and Development Program under project tracking code 08-LW-070.

*froula1@llnl.gov

[1] T. Tajima and J. M. Dawson, Phys. Rev. Lett. **43**, 267 (1979).
[2] C. E. Clayton *et al.*, Phys. Rev. Lett. **70**, 37 (1993).
[3] C. A. Coverdale *et al.*, Phys. Rev. Lett. **74**, 4659 (1995).
[4] A. Modena *et al.*, Nature (London) **377**, 606 (1995).
[5] D. Umstadter *et al.*, Science **273**, 472 (1996).
[6] V. Malka *et al.*, Science **298**, 1596 (2002).
[7] C. Geddes *et al.*, Nature (London) **431**, 538 (2004).
[8] J. Faure *et al.*, Nature (London) **431**, 541 (2004).
[9] S. Mangles *et al.*, Nature (London) **431**, 535 (2004).
[10] W. Lu, C. Huang, M. Zhou, W. B. Mori, and T. Katsouleas, Phys. Rev. Lett. **96**, 165002 (2006).
[11] W. Lu *et al.*, Phys. Plasmas **13**, 056709 (2006).
[12] G. Z. Sun *et al.*, Phys. Fluids **30**, 526 (1987).
[13] W. Lu *et al.*, Phys. Rev. ST Accel. Beams **10**, 061301 (2007).
[14] J. E. Ralph *et al.*, Phys. Rev. Lett. **102**, 175003 (2009).
[15] A. Thomas *et al.*, Phys. Rev. Lett. **98**, 095004 (2007).
[16] N. Hafz *et al.*, Nat. Photon. **2**, 571 (2008).
[17] F. Tsung *et al.*, Phys. Plasmas **13**, 056708 (2006).
[18] K. Nakamura *et al.*, Phys. Plasmas **14**, 056708 (2007).
[19] T. P. Rowlands-Rees *et al.*, Phys. Rev. Lett. **100**, 105005 (2008).
[20] A. E. Pak *et al.*, Phys. Rev. Lett. (to be published).
[21] V. V. Lozovoy *et al.*, Opt. Lett. **29**, 775 (2004).
[22] V. Malka *et al.*, Rev. Sci. Instrum. **71**, 2329 (2000).
[23] B. B. Pollock *et al.*, Proceedings of PAC09, Vancouver, Canada (2009) (to be published).
[24] I. Blumenfeld *et al.*, Nature (London) **445**, 741 (2007).
[25] N. Nakanii *et al.*, Rev. Sci. Instrum. **79**, 066102 (2008).
[26] B. C. Franke, Sandia National Laboratories Technical Report No. SAND2004-5172, 2005.
[27] R. A. Fonseca *et al.*, in ICCS 2002, LNCS 2331, edited by P. M. A. Sloot *et al.* (2002), pp. 342–351.
[28] J.-L. Vay, Phys. Rev. Lett. **98**, 130405 (2007).
[29] S. F. Martins *et al.* (to be published).